Highly Symmetric Group 13 Metal−Phosphinato Complexes: Multinuclear NMR (^{27}Al, ^{31}P, ^{71}Ga) Determination of Stability Constants at Low pH

Mark P. Lowe, Steven J. Rettig, and Chris Orvig*

Contribution from the Department of Chemistry, University of British Columbia, 2036 Main Mall, Vancouver, British Columbia, V6T 1Z1, Canada

Received May 15, 1996[⊗]

Abstract: An N_4O_3 tripodal tren-based (aminomethylene)phosphinato ligand tris(4-(phenylphosphinato)-3-methyl-3-azabutyl)amine (H_3ppma) has been synthesized, and its complexation properties with the group 13 metals Al, Ga, and In have been investigated. The molecular structure of the indium complex $[In(H_3ppma)_2](NO_3)_3 \cdot 3H_2O$ ($C_{60}H_{96}InN_{11}O_{24}P_6$) has been solved by X-ray methods; the complex crystallizes in the trigonal space group $R\bar{3}c$, with a = 18.984(3) Å, c = 36.256(5) Å, and Z = 6. The structure was solved by Patterson methods and was refined by full-matrix least-squares procedures to R = 0.040 (R_w = 0.039) for 1415 reflections with $I > 3\sigma(I)$. The structure of the bis-complex showed the ligand to coordinate in a tridentate manner through the three phosphinate oxygens, resulting in a bicapped octahedral structure of exact S_6 symmetry. The solved structure was of the *RRRSSS* diastereomer, where half of the molecule contained phosphorus atoms of *R* chirality and the other half contained phosphorus atoms of *S* chirality. The highly symmetric environment about the metal atoms produces a low electric field gradient at the metal nucleus leading to unusually narrow line widths in the ^{27}Al, ^{71}Ga, and ^{115}In NMR spectra. The aluminum complex $[Al(H_3ppma)_2](NO_3)_3 \cdot 2H_2O$ exhibited an extremely rare example of aluminum−phosphorus coupling in both the ^{31}P and ^{27}Al NMR spectra, where $^2J_{AlP}$ was shown from both spectra to be 6.7 Hz. The narrow line widths made the complexes amenable to stability constant studies via a combination of ^{27}Al, ^{71}Ga, and ^{31}P NMR spectroscopies (25 °C). The formation constants for In^{3+} ($\log \beta_2 \geq 5.4$), Ga^{3+} ($\log \beta_2 = 4.24$), and Al^{3+} ($\log \beta_1 = 0.93$, $\log \beta_2 = 3.45$) decrease by an order of magnitude as the group is ascended, consistent with increasing steric interactions of the phenyl groups as the two trisphosphinate ligands are crowded together in order to coordinate the smaller metal ions. Variable temperature ^{27}Al and ^{31}P NMR spectroscopic studies indicated the *RRRSSS* diastereomer to be rigid up to 55 °C in CD_3OD.

Introduction

Recent research interest in this group[1] has focused on the polydentate ligand coordination chemistry of the group 13 metals aluminum, gallium, and indium. Such work has stemmed from the concern over aluminum neurotoxicity[2] and from the use of gallium and indium radionuclides[3] in diagnostic radiopharmaceuticals. The use of tripodal ligands bearing aminophenolate groups has led to the discovery of a variety of possible coordination geometries[1,4] for complexes of group 13 metals and of lanthanides. In an effort to extend this chemistry, with the aim of providing complexes with potentially greater *in vivo* stability with respect to acid-catalyzed dissociation, different donor groups were sought, since the phenolic oxygens in the aforementioned ligand systems have high pK_a values (∼10) and therefore are readily protonated. Phosphinic acids were considered as suitable donors due to the very low pK_a of the phosphinic hydroxyl, and thus the chances of acid-catalyzed dissociation are greatly reduced. Coordination chemistry with phosphinic and phosphonic acids has received much attention over recent years, especially with amino acid analogs,[5] phosphonodipeptides,[6] and lanthanide complexes[7] which have received wide attention for their potential use as magnetic resonance imaging (MRI) contrast agents.[8] The chemistry of group 13 metals with these ligands, however, has not been explored to a great extent. The few investigations which have been undertaken have been concerned with the development of potential gallium and indium radiopharmaceuticals.[9,10] A model study on simple amino bisphosphonic acids was carried out by Roundhill and co-workers,[9] and recent work by the group of Parker[10] has led to preliminary *in vivo* studies of the gallium and indium complexes of macrocyclic ligands bearing methylenephosphinic acids.

Aluminum has received even less attention with respect to phosphonic/phosphinic acids; however, a fairly substantial body of work has been built up concerning the interaction of biologically relevant phosphates such as ATP with aluminum.[11]

* To whom correspondence should be addressed: fax: 604-822-2847; telephone: 604-822-4449; email ORVIG@CHEM.UBC.CA

⊗ Abstract published in *Advance ACS Abstracts,* September 1, 1996.

(1) (a) Wong, E.; Caravan, P.; Liu, S.; Rettig, S.; Orvig, C. *Inorg. Chem.* **1996**, *35*, 715. (b) Wong, E.; Liu, S.; Lügger, T.; Hahn, F. E.; Orvig, C. *Inorg. Chem.* **1995**, *34*, 93. (c) Liu, S.; Wong, E.; Karunaratne, V.; Rettig, S. J.; Orvig, C. *Inorg. Chem.* **1993**, *32*, 1756. (d) Liu, S.; Wong, E.; Rettig, S. J.; Orvig, C. *Inorg. Chem.* **1993**, *32*, 4268. (e) Liu, S.; Rettig, S. J.; Orvig, C. *Inorg. Chem.* **1992**, *31*, 5400.

(2) (a) Perl, D. P. *Environ. Health Perspect.* **1985**, *63*, 149. (b) Crapper-McLachlan, D. R. *Neurobiol. Aging* **1986**, *7*, 525. (c) Liss, L. *Aluminum Neurotoxicity*; Pathotox Publishers: Park Forest, IL, 1980.

(3) (a) Welch, M. J.; Moerlein, S. M. In *Inorganic Chemistry in Biology and Medicine*; Martell, A. E., Ed.; American Chemical Society: Washington, DC, 1980; p 121. (b) Green, M. A.; Welch, M. J. *Nucl. Med. Biol.* **1989**, *16*, 435. (c) Zhang, Z.; Lyster, D. M.; Webb, G. A.; Orvig, C. *Nucl. Med, Biol.* **1992**, *19*, 327.

(4) Yang, L.-W.; Liu, S.; Wong, E.; Rettig, S. J.; Orvig, C. *Inorg. Chem.* **1995**, *34*, 2164.

(5) (a) Kiss, T.; Lázár, I.; Kafarski, P. *Met.-Based Drugs* **1994**, *1*, 247. (b) Jezowska-Bojczuk, M.; Kiss, T.; Kozlowski, H.; Decock, P.; Barycki, J. *J. Chem. Soc., Dalton Trans.* **1994**, 811.

(6) (a) Hermann, P.; Lukeš, I. *J. Chem. Soc., Dalton Trans.* **1995**, 2605. (b) Hermann, P.; Lukeš, I.; Vojtíšek, P.; Císarová, I. *J. Chem. Soc., Dalton Trans.* **1995**, 2611.

(7) (a) Lázár, I.; Sherry, A. D.; Ramasamy, R.; Brücher, E.; Kiraly, R. *Inorg. Chem.* **1991**, *30*, 5016. (b) Lázár, I.; Ramasamy, R.; Brücher, E.; Geraldes, C. F. G. C.; Sherry, A. D. *Inorg. Chim. Acta* **1992**, *195*, 89.

(8) (a) Aime, S.; Batsanov, A. S.; Botta, M.; Howard, J. A. K.; Parker, D.; Senanayake, K.; Williams, G. *Inorg. Chem.* **1994**, *33*, 4696. (b) Aime, S.; Botta, M.; Parker, D.; Williams, J. A. G. *J. Chem. Soc., Dalton Trans.* **1995**, 2259.

(9) Bollinger, J. E.; Roundhill, D. M. *Inorg. Chem.* **1993**, *32*, 2821.

(10) Cole, E.; Copley, R. C. B.; Howard, J. A. K.; Parker, D.; Ferguson, G.; Gallagher, J. F.; Kaitner, B.; Harrison, A.; Royle, L. *J. Chem. Soc., Dalton Trans.* **1994**, 1619.

S0002-7863(96)01633-2 CCC: $12.00

In some of these studies, combined $^{27}Al/^{31}P$ NMR spectroscopic techniques have been employed to investigate phosphate−aluminum interactions, and in the recent work of Detellier and co-workers,[11a] equilibrium constants have been obtained from ^{31}P NMR spectra. ^{27}Al NMR spectroscopy is a useful probe for these systems, despite the quadrupolar nature of aluminum ($I = {}^5/_2$); the 100% abundance and reasonable receptivity can sometimes lead to resonances of fairly narrow line width. A broadening occurs in some of the ^{31}P NMR signals which cannot be attributed entirely to exchange processes, a broadening which was in some cases[11b,e] unresolved phosphorus−aluminum coupling.

Gallium possesses two NMR active nuclei, ^{69}Ga and ^{71}Ga, both with a spin of $I = {}^3/_2$. ^{69}Ga is the more abundant isotope (60.4 vs 39.6%); however, ^{71}Ga is the nucleus of choice for NMR studies due to its higher receptivity and smaller quadrupole moment. Even so, gallium is even less well-suited to study by NMR than is ^{27}Al, since broad resonances are commonly observed due to rapid relaxation of the quadrupolar nuclei, especially when the nucleus is interacting with asymmetric electric field gradients. Generally, all that can be gleaned from a ^{71}Ga NMR study is a clue to the geometry of the complex, which dictates chemical shift (*i.e.*, octahedral vs tetrahedral) and the symmetry of a complex, since the line width is extremely sensitive to molecular symmetry about the nucleus. In light of these factors, gallium NMR spectroscopy has been of little use outside the realm of the solid state.[12] In spite of the unwelcoming nuclear properties of gallium, it will be shown herein that, given a highly symmetric environment, ^{71}Ga NMR can prove to be a useful tool in solution studies of its complexes.

Initial complexation studies with tris(4-(phenylphosphinato)-3-methyl-3-azabutyl)amine (H_3ppma) revealed a propensity to form stable 2:1 (L:M) complexes of octahedral geometry, each ligand coordinating through three $P-O^-$ groups. These complexes form at extremely low pH (<2), a regime in which potentiometry is of no use for studying the solution chemistry. At higher pH, precipitation of the complexes occurs. Even if the complexes were to remain in solution, no protons are displaced in the complexation step and the complex formation would remain invisible to potentiometry. Other methods were sought to determine the stability constants, with NMR spectroscopy proving to be the only suitable tool. The complexes are 6-fold symmetric, as shown in the ^1H and ^{31}P NMR spectra. Measurement of the ^{27}Al, ^{71}Ga, and ^{115}In NMR spectra of the respective isolated complexes resulted in the observation of unusually narrow line widths. Because of this amenability to NMR study, a combined $^{31}P-^{27}Al/^{71}Ga$ NMR investigation was carried out in order to determine the formation constants of the 2:1 complexes at low pH. These investigations led to the discovery for the aluminum complex of well-resolved $^2J_{AlP}$ coupling in both ^{27}Al and ^{31}P NMR spectra which is unprecedented for this type of coordination complex.

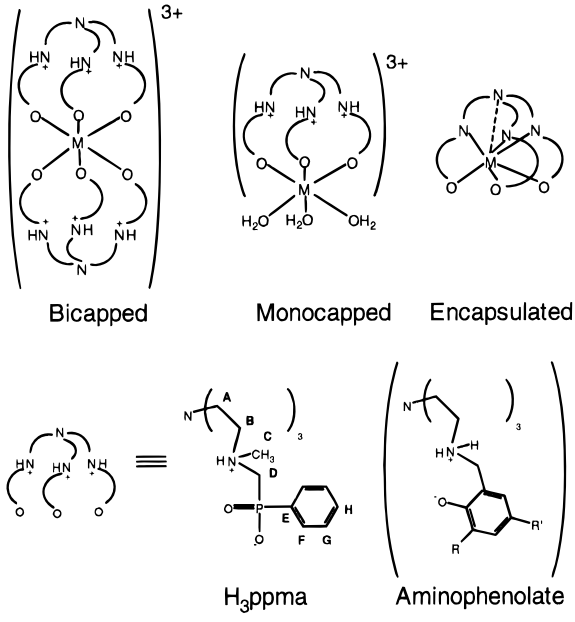

Experimental Section

Materials. Tris(2-aminoethyl)amine (tren), lithium aluminum hydride, phenylphosphinic acid, and hydrated gallium and indium nitrates were obtained from Aldrich. Formaldehyde solution (37% w/w) was obtained from Fisher, and ethyl chloroformate was from Eastman. Hydrated aluminum nitrate, aluminum chloride, and indium chloride were obtained from Mallinckrodt, Anachemia, and Alfa, respectively. D_2O was obtained from ISOTEC, and methanol-d_4 (CD_3OD) was from Cambridge Isotope Laboratories.

Instruments. NMR spectra were recorded on Bruker AC-200E ($^1H-^1H$ COSY, $^{31}P\{H\}$) and Varian XL300 (^1H, $^{13}C\{H\}$, ^{27}Al, $^{31}P\{H\}$, ^{71}Ga and ^{115}In) spectrometers. Metal NMR spectra were recorded in CD_3OD and are referenced to 0.1 M $M(NO_3)_3$ in 6 M HNO_3. ^{31}P NMR spectra were referenced to external 85% H_3PO_4. Mass spectra were obtained on a Kratos Concept II H32Q (Cs^+, LSIMS) instrument with thioglycerol as the matrix. Infrared spectra were obtained as KBr disks in the range of 4000−400 cm^{-1} on a Galaxy Series 5000 FTIR spectrometer. UV spectra were recorded on a Shimadzu UV-2100 spectrophotometer. Analyses for C, H, and N were performed by Mr. Peter Borda in this department.

Tris(3-azabutyl)amine. This amine was synthesized according to published methods, by the reaction of tren with ethyl chloroformate followed by the reduction of the resulting carbamate with lithium aluminum hydride to give the tri-*N*-methylated amine.[13]

Tris(4-(phenylphosphinato)-3-methyl-3-azabutyl)amine Trihydrochloride Monohydrate (H_3ppma·3HCl·H_2O). This compound was prepared using a modification of the Moedritzer−Irani[14] synthesis of (aminomethylene)phosphonic acids. Phenylphosphinic acid (2.13 g, 14.99 mmol) and tris(3-azabutyl)amine (0.91 g, 4.83 mmol) were dissolved in distilled water (20 mL). After slow addition of 37% HCl (20 mL), the temperature of the stirred solution was raised to reflux (∼110 °C) and 37% w/w aqueous formaldehyde (2.44 g, 30.09 mmol) was added dropwise over 30 min. The reaction was refluxed for a further 5 h, after which time the HCl−H_2O solvent mixture was concentrated under vacuum almost to dryness. The resulting syrup was taken up in ethanol (100 mL), and acetone (900 mL) was added to give a cloudy solution which was cooled and then filtered. A white, highly hygroscopic powder was obtained; this was taken up in water, and the solvent removed once more. Drying under vacuum for 12 h gave a glassy, slightly hygroscopic solid in a 2.40 g yield (64%): MS (+LSIMS), *m/z* 651 ($[L + 1]^+$, $[C_{30}H_{46}N_4O_6P_3]^+$); IR ($cm^{-1}$, KBr disk) 3410, 2460 (bs, ν_{NH}, ν_{OH}), 1645 (w, δ_{NH}), 1438 (s, ν_{PPh}), 1206, 1131, 957 (ν_{PO}), 740, 685, 599 (ν_{PC}, ν_{PPh}): UV (λ_{max}, nm (ϵ, M^{-1} cm^{-1}), pH = 1.5) 258 (1375), 264 (1833), 271 (1512). Anal. Calcd (found) for $C_{30}H_{45}N_4O_6P_3$·3HCl·H_2O: C, 46.31 (46.58); H, 6.48 (6.48); N, 7.20 (7.31). Potentiometric studies were consistent with this molecular weight. ^1H, ^{13}C, and ^{31}P NMR spectral data are listed in Tables 1 and 2.

Synthesis of Metal Complexes. ^1H, ^{13}C, and ^{31}P NMR data for the complexes are given in Tables 1 and 2.

[Al(H_3ppma)$_2$][NO_3]$_3$·2H_2O. The pH of an aqueous solution (3 mL) of H_3ppma·3HCl·H_2O (0.050 g, 0.064 mmol) and $Al(NO_3)_3$·9H_2O (0.012 g, 0.032 mmol) was raised to 1.7 using 3M NaOH. Colorless

(11) (a) Dellavia, I.; Blixt, J.; Dupressoir, C.; Detellier, C. *Inorg. Chem.* **1994**, *33*, 2823. (b) Karlik, S. J.; Elgavish, G. A.; Eichhorn, G. L. *J. Am. Chem. Soc.* **1983**, *105*, 602. (c) Feng, Q.; Waki, H.; Kura, G. *Polyhedron* **1991**, *10*, 1527. (d) Karlik, S. J.; Elgavish, G. A.; Pillai, R. P.; Eichhorn, G. L. *J. Magn. Reson.* **1982**, *49*, 164. (e) Bock, J. L.; Ash, D. E. *J. Inorg. Biochem.* **1980**, *13*, 105.

(12) (a) Hinton, J. F.; Briggs, R. W. *NMR and the Periodic Table*; Harris, R. K., Mann, B. E., Eds.; Academic: London, 1978; pp 279−303. (b) Akitt, J. W. *Prog. Nucl. Magn. Reson. Spectros.* **1989**, *21*, 1.

(13) Schmidt, H.; Lensink, C.; Xi, S. K.; Verkade, J. G. *Z. Anorg. Allg. Chem.* **1989**, *578*, 75.

(14) Moedritzer, K.; Irani, R. R. *J. Org. Chem.* **1966**, *31*, 1603.

Table 1. ^{1}H NMR Spectral Data (CD_3OD) for H_3ppma and Its Group 13 Metal Complexes[a,b]

	H_3ppma	$[Al(H_3ppma)_2]^{3+}$	$[Ga(H_3ppma)_2]^{3+}$	$[In(H_3ppma)_2]^{3+}$
H_A	3.11	3.12 (−15.4, 10.3)	3.11 (−15.5, 10.4)	3.19 (−15.3, 10.4)
$H_{A'}$		2.49 (4.1)	2.46 (4.1)	2.40 (4.2)
H_B	3.70	4.67 (−13.3)	4.62 (−13.3)	4.63 (−13.1)
$H_{B'}$		2.94	2.90	3.02
H_C	3.06	2.96	2.99	3.02
H_D	3.75(8.3)	2.07 (−13.9, 11.2)	2.07 (−13.7, 11.2)	2.19 (−13.6, 10.8)
$H_{D'}$		2.68 (∼1)	2.72 (∼1)	2.90 (∼1)
H_F	7.90	7.72	7.68	7.54
H_G	7.55	7.39	7.37	7.35
H_H	7.65	7.47	7.47	7.46

[a] Numbers in parentheses correspond to coupling constants in hertz (for $H_A = {}^2J_{AA'}$, ${}^3J_{AB}$; $H_{A'} = {}^3J_{A'B'}$; $H_B = {}^2J_{BB'}$; $H_D = {}^2J_{DD'}$, ${}^2J_{DP}$; $H_{D'} = {}^2J_{D'P}$). [b] For labeling, see the structure for H_3pmma.

Table 2. ^{13}C{H} and ^{31}P NMR Spectral Data (CD_3OD) for H_3ppma and its Group 13 Metal Complexes[a,b]

	H_3ppma	$[Al(H_3ppma)_2]^{3+}$	$[Ga(H_3ppma)_2]^{3+}$	$[In(H_3ppma)_2]^{3+}$
C_A	49.4	52.5	52.4	52.1
C_B	56.2	57.7	58.0	58.5
C_C	45.0 (5.4)	47.5 (10.1)	47.4 (9.5)	47.7 (8.9)
C_D	56.2 (95.0)	57.3 (101.5)	57.6 (99.1)	58.0 (98.3)
C_E	133.0 (139.8)	135.0 (142.3)	135.4 (141.3)	135.3 (141.2)
C_F	132.7 (10.6)	133.9 (9.9)	134.0 (9.9)	133.8 (10.2)
C_G	130.1 (13.3)	129.2 (12.8)	129.2 (12.7)	129.0 (13.1)
C_H	134.3 (2.6)	133.1 (2.3)	133.1 (2.6)	133.1 (2.2)
P	26.0	13.2	15.0	17.4

[a] Numbers in parentheses correspond to coupling constants in hertz (where carbon C = ${}^3J_{PC}$, D = ${}^1J_{PC}$, E = ${}^1J_{PC}$, F = ${}^2J_{PC}$, G = ${}^3J_{PC}$, H = ${}^4J_{PC}$). [b] For labeling, see the structure for H_3pmma.

prisms were deposited after 24 h. These prisms were filtered and dried under vacuum to yield 0.020 g (39%): MS (+LSIMS), *m/z* 1325 ($[ML_2 - 2H]^+$, $[C_{60}H_{88}N_8O_{12}P_6Al]^+$), 675 ($[ML - 2H]^+$, $[C_{30}H_{43}N_4O_6P_3Al]^+$), 663 ($[ML_2 - H]^{2+}$, $[C_{60}H_{89}N_8O_{12}P_6Al]^{2+}$), 651 ($[L + 1]^+$, $[C_{30}H_{46}N_4O_6P_3]^+$); IR (cm^{-1}, KBr disk) 3435, 2426 (bs, ν_{NH}, ν_{OH}), 1653 (w, δ_{NH}), 1458 (s, ν_{PPh}), 1382 (s, ν_{NO_3}), 1194, 1138, 1082 (ν_{PO}), 746, 719, 582, 562 (ν_{PC}, ν_{PPh}). ^{27}Al NMR: δ −12.9 ($W_{1/2}$ = 23.0 Hz). Anal. Calcd (found) for $C_{60}H_{90}AlN_{11}O_{21}P_6\cdot 2H_2O$: C, 46.49 (46.62); H, 6.11 (6.15); N, 9.94 (9.85).

$[Ga(H_3ppma)_2][NO_3]_3\cdot 3H_2O$. The pH of an aqueous solution (3 mL) of H_3ppma·3HCl·H_2O (0.050 g, 0.064 mmol) and $Ga(NO_3)_3\cdot 9H_2O$ (0.013 g, 0.031 mmol) was raised to 2.0 using 3M NaOH. Colorless prisms were deposited after 1 week. these prisms were filtered and dried under vacuum to yield 0.024 g (48%): MS (+LSIMS), *m/z* 1367 ($[ML_2 - 2H]^+$, $[C_{60}H_{88}N_8O_{12}P_6Ga]^+$), 717 ($[ML - 2H]^+$, $[C_{30}H_{43}N_4O_6P_3Ga]^+$), 685 ($[ML_2 - H]^{2+}$, $[C_{60}H_{89}N_8O_{12}P_6Ga]^{2+}$), 651 ($[L + 1]^+$, $[C_{30}H_{46}N_4O_6P_3]^+$); IR (cm^{-1}, KBr disk) 3445, 2506 (bs, ν_{NH}, ν_{OH}), 1637 (w, δ_{NH}), 1382 (s, ν_{NO_3}), 1462 (s, ν_{PPh}), 1190, 1134, 1070 (ν_{PO}), 742, 718, 578, 558 (ν_{PC}, ν_{PPh}); ^{71}Ga NMR δ −62.3 ($W_{1/2}$ = 50.0 Hz). Anal. Calcd (found) for $C_{60}H_{90}GaN_{11}O_{21}P_6\cdot 3H_2O$: C, 44.73 (45.00); H, 6.01 (6.00); N, 9.56 (9.55).

$[In(H_3ppma)_2][NO_3]_3\cdot 3H_2O$. The pH of an aqueous solution (6 mL) of H_3ppma·3HCl·H_2O (0.175 g, 0.225 mmol) and $In(NO_3)_3\cdot 9H_2O$ (0.052 g, 0.110 mmol) was raised to 2.2 using 3 M NaOH. Colorless prisms deposited after 1 h; these prisms were filtered and dried under vacuum to yield 0.130 g (70%): MS (+LSIMS), *m/z* 1413 ($[ML_2 - 2H]^+$, $[C_{60}H_{88}N_8O_{12}P_6In]^+$), 763 ($[ML - 2H]^+$, $[C_{30}H_{43}N_4O_6P_3In]^+$), 708 ($[ML_2 - H]^{2+}$, $[C_{60}H_{89}N_8O_{12}P_6In]^{2+}$), 651 ($[L + 1]^+$, $[C_{30}H_{46}N_4O_6P_3]^+$); IR (cm^{-1}, KBr disk) 3424, 2574 (bs, ν_{NH}, ν_{OH}), 1643 (w, δ_{NH}), 1438 (s, ν_{PPh}), 1382 (s, ν_{NO_3}), 1191, 1134, 1066 (ν_{PO}), 742, 718, 578, 558 (ν_{PC}, ν_{PPh}); ^{115}In NMR δ −14.7 ($W_{1/2}$ = 1630 Hz). Anal. Calcd (found) for $C_{60}H_{90}InN_{11}O_{21}P_6\cdot 3H_2O$: C, 43.51 (43.37); H, 5.84 (5.89); N, 9.30 (9.36).

NMR Measurements (Equilibrium Constant Studies). ^{27}Al, ^{71}Ga, ^{115}In, and ^{31}P NMR spectra were recorded on a Varian XL-300 spectrometer in H_2O. ^{27}Al spectra were recorded at an operating frequency of 78.16 MHz with a spectral window of 10 KHz; accumulating ∼1000 transients with a pulse width of 15 μs (90°) and an acquisition time of 0.4 s gave 8000 data points. All spectra were referenced to 0.1 M $Al(NO_3)_3$ in 6 M HNO_3. ^{71}Ga spectra were recorded at an operating frequency of 91.48 MHz with a spectral window of 10 KHz (transmitter offset = −14 KHz); accumulating ∼1500 transients with a pulse width of 19 μs (90°) and an acquisition time of 0.4 s gave 8000 data points. All spectra were referenced to 0.1 M $Ga(NO_3)_3$ in 6 M HNO_3. ^{115}In spectra were recorded at an operating frequency of 65.74 MHz with a spectral window of 50 KHz (transmitter offset = −25 KHz); accumulating ∼2000 transients with a pulse width of 20 μs (90°) and an acquisition time of 0.15 s gave 15000 data points. All spectra were referenced to 0.1 M $In(NO_3)_3$ in 6 M HNO_3. ^{31}P{H} spectra were recorded at an operating frequency of 121.0 MHz, a spectral window of 10 KHz, accumulation of ∼500 transients, a pulse width of 8 μs, an acquisition time of 0.16 s, and a delay of 1.6 s. These conditions gave 3200 data points. All spectra were referenced to 85% H_3PO_4. The pulse delay for a representative sample was varied, and the relative integrals were compared. These integrals were found to be consistent for delay times > 1.0 s; therefore a delay of 1.6 s was employed in ^{31}P NMR to ensure full relaxation of all species.

The pH of the solutions studied was measured with a Fisher Accumet 805NP pH meter employing a Canadawide Scientific Ag/AgCl combination microelectrode and was adjusted to pH = 1.5 using 1 M HCl or 1 M NaOH. Metal ion stock solutions were prepared from the hydrates of $AlCl_3$ (48.5 mM), $Ga(NO_3)_3$ (49.6 mM), and $InCl_3$ (49.7 mM) and were analyzed by passage through a cation exchange column (Rexyn 101-H) followed by titration of the resulting eluent with standardized NaOH (each M^{3+} liberating $3H^+$). The H_3ppma stock solution (198.1 mM) was analyzed by potentiometric titration as a diluted 1.5 mM solution (three times). The amount of base added between two inflection points (highlighted on a plot of δ pH/δ Vol) is equivalent to the concentration of the H_3ppma; the hygroscopic nature of H_3ppma makes this a more accurate measure of concentration than one based on weight. All solutions contained a fixed amount of M^{3+} (∼25 mM) with the ligand concentration varied ($[L]_T/[M]_T = 4-0.25$). Solutions were made up to a volume of 0.8 mL, and the pH was adjusted to 1.5. The solutions were allowed to equilibrate for 48 h prior to the spectra being collected. The respective peak integrals enabled a quantitative measure to be obtained of free ligand ([L]), bound ligand ([ML] and 2[ML_2]), free metal ([M^{3+}]), and bound metal ([ML] and [ML_2]). The knowledge of these values allowed $\bar{n}$, the ratio of bound ligand to total metal, to be calculated ($\bar{n} = ([L]_T - [L])/[M]_T$). A plot of $\bar{n}$ vs [L] resulted in a curve from which the variables β_1 and β_2 for Al(III) and β_2 for Ga(III) could be calculated using computer curve-fitting software.

Potentiometric Measurements. Potentiometric measurements of tris(3-azabutyl)amine and H_3ppma were performed using the method described elsewhere.[15] The temperature of the solutions (1.1 and 1.5 mM, respectively) was kept constant at 25.0 ± 0.1 °C, and the ionic strength was fixed at μ = 0.16 M NaCl.

(15) Caravan, P.; Hedlund, T.; Liu, S.; Sjöberg, S.; Orvig, C. *J. Am. Chem. Soc.* **1995**, *117*, 11230.

Table 3. Selected Crystallographic Data for $[In(H_3ppma)_2](NO_3)_3 \cdot 3H_2O$

formula	$C_{60}H_{96}InN_{11}O_{24}P_6$
mol wt, amu	1656.14
crystal system	trigonal
space group	$R\bar{3}c$
a, Å	18.984(3)
c, Å	36.256(5)
V, Å^3	11315(3)
Z	6
ρ_{calc}, g/cm^3	1.458
T, °C	21
radiation λ, Å	Cu 1.54178
μ, cm^{-1}	44.00
transm factors	0.58−1.00
R (F)[a]	0.040
R_w (F)[a]	0.039

[a] $R = \sum||F_o| - |F_c||/\sum|F_o|$; $R_w = (\sum w(|F_o| - |F_c|)^2/\sum w|F_o|^2)^{1/2}$.

X-ray Crystallographic Analyses of $[C_{60}H_{90}InN_8O_{12}](NO_3)_3 \cdot 3H_2O$. Selected crystallographic data appear in Table 3. The final unit-cell parameters were obtained by least-squares on the setting angles for 25 reflections with $2\theta = 21.8-43.9$. The intensities of three standard reflections, measured every 200 reflections throughout the data collection, remained constant. The data were processed[16] and corrected for Lorentz and polarization effects and absorption (empirical, based on azimuthal scans).

The structure of $[C_{60}H_{90}InN_8O_{12}](NO_3)_3 \cdot 3H_2O$ was solved by the Patterson method. The structure analysis was initiated in the centrosymmetric space group $R\bar{3}c$ on the basis of the E-statistics, this choice being confirmed by subsequent calculations. The nitrate anions and water molecules were modeled as (1:1) disordered about a point of S_6 symmetry. Because of thermal motion and near overlap of disordered components, the nitrate groups deviate from ideal geometry. Refinement of the structure in the noncentrosymmetric space group $R3c$ failed to resolve the disorder. All non-hydrogen atoms of were refined with anisotropic thermal parameters. Hydrogen atoms were fixed in calculated positions (N−H = 0.91 Å, C−H = 0.98 Å, $B_H = 1.2\ B_{bonded\ atom}$). A correction for secondary extinction (Zacharaisen type) was applied, the final value of the extinction coefficient being 6.3(4) × 10^{-8}. Neutral atom scattering factors for all atoms[17] and anomalous dispersion corrections for the non-hydrogen atoms[18] were taken from the *International Tables for X-Ray Crystallography*. Selected bond lengths and bond angles appear in Table 4. Complete tables of crystallographic data, final atomic coordinates and equivalent isotropic thermal parameters, anisotropic thermal parameters, bond lengths, bond angles, torsion angles, intermolecular contacts, and least-squares planes are included as supporting information.

Results

H_3ppma. The ^{1}H NMR spectrum of H_3ppma showed the expected simple spectrum, with the ethylenic protons giving broad resonances due to the fluxionality of the molecule. The methylenic resonance appears as a sharp doublet due to coupling to phosphorus ($^2J_{PH} = 8.3$ Hz). The aromatic hydrogens give rise to a complex overlapping multiplet due to coupling to both hydrogens and phosphorus.

Three pK_a values determined potentiometrically for the ligand (pK_{a1} = 8.82(6), pK_{a2} = 7.10(6), pK_{a3} = 6.43(2) (at the 3σ confidence level)), corresponding to the sequential deprotonation of the three pendant tertiary ammonium nitrogens, were confirmed by a variable pD ^{1}H and ^{31}P NMR titration. The apical nitrogen in such tren-based ligands is known to be highly acidic.[19] The pK_a values of phosphinate oxygens are too low to be measured potentiometrically and are widely agreed to be ≤1.[5,6] The three measurable pK_a values of tren are pK_{a1} = 10.13, pK_{a2} = 9.43, and pK_{a3} = 8.41.[20] The three pK_a values determined potentiometrically for tris(3-azabutyl)amine (pK_{a1} = 10.44(12), pK_{a2} = 9.70(3), pK_{a3} = 8.41(6) (at the 3σ confidence level)), corresponding to the sequential deprotonation of the 3 pendant secondary ammonium nitrogens are as expected, (*i.e.*, slightly higher than those of tren due to the inductive effect of the methyl groups). The lowering of the pK_a values of the parent amine on derivatization is commonly observed for (aminomethylene)phosphonic and -phosphinic acids and is attributed to the electron-withdrawing effect of the phosphinate moiety which renders the nitrogens less basic.[5] The pK_a values correlate well with the amine pK_a values of the related carboxylate derivative, tris(4-carboxy-3-methyl-3-azabutyl)amine[19] (pK_{a1} = 9.97, pK_{a2} = 9.24, and pK_{a3} = 8.08) and show the expected dependence on electron-withdrawing effects of the attached group, where the amine pK_a values for RPO_2^- < CO_2^-.[5] This moderate basicity precludes complexation of the nitrogens to the group 13 metals at the low pH used in this study and dictates binding exclusively through the highly acidic oxygens. This is contrary to the studies by Parker and co-workers[10] on macrocyclic polyamines bearing phenylphosphinate groups, where complexation at low pH was observed by both nitrogen and oxygen donors. This is presumably facilitated by the relatively high acidity of one of the nitrogens, induced by the close proximity of the three nitrogens in the macrocyclic ring (*c.f.*, the pK_a values obtained for the tris(methylenephosphonate) of triazacyclononane as determined by the Sherry group (pK_a values for the three nitrogens are 11.7, 9.1, and 0.9).[21]

Table 4. Selected Bond Lengths (Å) and Angles (deg)* for $[In(H_3ppma)_2][NO_3]_3 \cdot 3H_2O$

Lengths

atom	atom	distance	atom	atom	distance
In(1)	O(1)	2.117(3)	P(1)	O(1)	1.501(3)
P(1)	O(2)	1.491(3)	P(1)	C(4)	1.835(5)
P(1)	C(5)	1.778(5)	N(1)	C(1)	1.470(5)
N(2)	C(2)	1.512(6)	N(2)	C(3)	1.492(6)
N(2)	C(4)	1.495(6)			

Angles

atom	atom	atom	angle	atom	atom	atom	angle
O(1)	In(1)	O(1)$^{(1)}$	90.0(1)	O(1)	In(1)	O(1)$^{(2)}$	180.0
O(1)	In(1)	O(1)$^{(3)}$	90.0(1)	O(1)	P(1)	O(2)	119.6(2)
O(1)	P(1)	C(4)	102.6(2)	O(1)	P(1)	C(5)	109.5(2)
O(2)	P(1)	C(4)	109.9(2)	O(2)	P(1)	C(5)	110.7(2)
C(4)	P(1)	C(5)	102.9(2)	In(1)	O(1)	P(1)	141.3(2)
C(1)	N(1)	C(1)$^{(1)}$	108.0(3)	C(2)	N(2)	C(3)	111.2(4)
C(2)	N(2)	C(4)	111.8(4)	C(3)	N(2)	C(4)	110.2(4)
N(1)	C(1)	C(2)	112.6(4)	N(2)	C(2)	C(1)	113.2(4)
P(1)	C(4)	N(2)	112.1(3)	P(1)	C(5)	C(6)	121.6(4)
P(1)	C(5)	C(10)	120.1(4)				

[a] (1) $-y, x - y, z$; (2) $-x, -y, 1 - z$; (3) $y, -x + y, 1 - z$.

Metal Complexes. The facile synthesis of the hydrated $[M(H_3ppma)_2][NO_3]_3$ complexes (M = Al, Ga, In) was achieved by slight adjustment of the pH of an aqueous solution of the metal nitrate and H_3ppma in a 1:2 stoichiometry. The hydrophobicity of the phenyl rings no doubt facilitates the precipitation of the complexes. The IR spectra of these complexes are superimposable, with the expected ν_{NO_3} and ν_{PO} stretches being prominent with ν_{NO_3} being typical of noncoordinated nitrate. The LSIMS (+) mass spectra show molecular ions $[ML_2 - 2H]^+$ at the appropriate *m/z* for the bicapped species, along with the monoligand species at $[ML - 2H]^+$. This monoligand peak

(16) *teXsan*; Crystal Structure Analysis Package (1985 & 1992); Molecular Structure Corporation: The Woodlands, TX.

(17) *International Tables for X-Ray Crystallography*; Kynoch Press: Birmingham, England, 1974; Vol. IV, pp 99−102.

(18) *International Tables for Crystallography*; Kluwer Academic Publishers: Boston, MA, 1992; Vol. C, pp 200−206.

(19) Geraldes, C. F. G. C.; Brücher, E.; Cortes, S.; Koenig, S. H.; Sherry, A. D. *J. Chem. Soc., Dalton Trans.* **1992**, 2517.

(20) Martell, A. E.; Smith, R. M. *Critical Stability Constants*; Plenum: New York, 1974−1989; Vols. 1−6.

(21) Geraldes, C. F. G. C.; Sherry, A. D.; Cacheris, W. P. *Inorg. Chem.* **1989**, *28*, 3336.

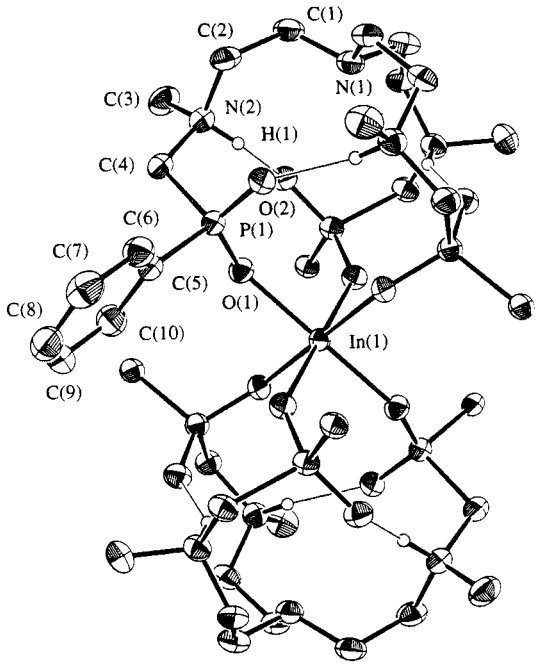

Figure 1. ORTEP representation of the X-ray crystal structure of [In(H$_3$ppma)$_2$](NO$_3$)$_3$·3H$_2$O (25% probability thermal ellipsoids). Only one phenyl group is shown for clarity.

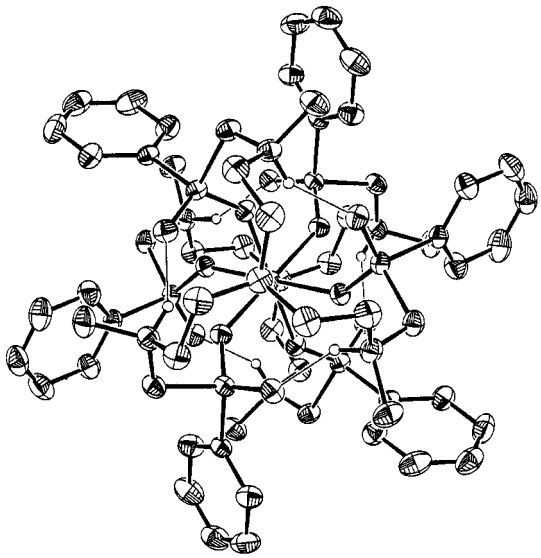

Figure 2. ORTEP representation of the X-ray crystal structure of [In(H$_3$ppma)$_2$](NO$_3$)$_3$·3H$_2$O (25% probability thermal ellipsoids). The view is approximately down the 3-fold axis.

is evidently derived from the parent bisligand bicapped species, since elemental analysis and NMR show no trace of monoligand complexes in the isolated solids. Interestingly, peaks for the dipositive molecular ion $[ML_2 - H]^{2+}$ are observed in all cases. Finally, peaks due to the ligand $[L + H]^+$ are always observed at $m/z = 651$.

X-ray Crystal Structure of [In(H$_3$ppma)$_2$][NO$_3$]$_3$·3H$_2$O. The crystals were isolated as colorless prisms and crystallized in the space group $R\bar{3}c$. ORTEP drawings of the $[In(H_3ppma)_2]^{3+}$ cation are shown in Figures 1 and 2, and selected bond distances and angles are listed in Table 4. The structure is of a bicapped nature similar to that observed for the bisligand tren-based aminophenolate lanthanide complexes previously reported by this group.[22] An arresting feature is the exact S_6 symmetry of the complex, a factor which plays an important role in the success of the NMR studies to be discussed later. The trans O−In−O angle is crystallographically imposed at 180.0, and both cis O−In−O angles are 90.0(1), resulting in perfect octahedral geometry. This suggests that the ionic radius of In^{3+} (0.800 Å) is the ideal size to accommodate this ligand in a bicapped manner. In−O distances of 2.117(3) Å are within the expected range. One important consequence of the S_6 symmetry is the stereochemistry at the phosphorus atoms. As mentioned earlier, on coordination to the metal ion, the phosphorus atoms are rendered chiral, with half of the bicapped structure possessing all *R* chirality and half all *S*. This opposing *RRRSSS* chirality generates the symmetry and is indeed necessary to accommodate the six bulky phenyl rings because, once the phosphinates coordinate, the phenyls completely engulf the coordination sphere. Only two diastereomers are sterically possible since the chirality of the phosphinate groups must be complimentary (*i.e.*, each one must be opposed by one of opposite chirality to allow the phenyl rings to slide in between each other). One diastereomer is the observed *RRRSSS* and the only other possible diastereomer is the one in which phosphorus atoms are *RRSSSR*. There is evidence for the existence of the latter in the NMR studies to be discussed later, but it is clear that in the crystals only the *RRRSSS* diastereomer is present. Another point of interest in this structure is the highly ordered intramolecular hydrogen bonding from the protonated nitrogen N(2) to the phosphinate oxygen O(2) on an adjacent arm, where H···O = 1.84 Å (N···O = 2.659(3) Å) and N−H···O = 149°. This is likely an important feature in maintaining the rigidity of the complex, and hence maintaining the high symmetry, by holding the left- and right-handed screws of the two hemispheres of the molecule.

^{1}H, ^{13}C, ^{31}P, ^{27}Al, ^{71}Ga, and ^{115}In NMR of [M(H$_3$ppma)$_2$][NO$_3$]$_3$. The ^{1}H NMR spectra of the three complexes in CD_3OD were almost identical, with the only differences being slight variations in chemical shift as the group is descended (Table 1). Upon coordination to the metal ions, the spectrum of the ligand changes markedly. The S_6 symmetric nature of the complex renders the arms of the ligand equivalent, and thus, ten resonances are observed. The free ligand showed only seven resonances, the additional three in the complex arise from the rigidity of the structure. The ethylenic hydrogens form an AA′BB′ spin system consisting of a distinct resonance corresponding to each of the four hydrogens. This is a pattern similar to those observed in macrocyclic[10] and small heterocyclic[23,24] ring structures, whereby the ethylenic hydrogens are locked in an axial−equatorial type conformation. This rigidity also gives rise to the nonequivalence of the methylenephosphinic hydrogens (NCH_2P), one of these hydrogens occurring at higher frequency from deshielding caused by its proximity to the hydrogen-bonded P═O.

The ^{1}H assignments are shown in Figure 3, which also shows the spectrum of the aluminum complex. The large shift of hydrogen H_B to a much higher frequency than the others is a result of the deshielding effects imparted by P═O. The X-ray structure of the indium complex reveals this hydrogen to be close to P═O. The remaining ethylenic hydrogens can be assigned from their respective coupling patterns and from the 2D ^{1}H−^{1}H COSY spectrum and occur in an almost identical pattern to that observed by Parker and co-workers[10] for the gallium complex of tris(methylene(phenyl)phosphinate) of triazacyclononane. The Newman projection in Figure 3 shows the arrangement of these hydrogens. The vicinal couplings between sets of hydrogens consist of one $J_g^{g'}$, two J_g^g, and one J_t^g type coupling. An estimation of the magnitude of the

(22) Liu, S.; Yang, L.-W.; Rettig, S. J.; Orvig, C. *Inorg. Chem.* **1993**, *32*, 2773.

(23) Lowe, M. P.; Lockhart, J. C.; Matthews, C. J.; Clegg, W.; Elsegood, M. R. J.; Horsburgh, L. *J. Chem. Soc., Perkin Trans. 2* **1994**, 1957.

(24) Günther, H. *NMR Spectroscopy*; John Wiley and Sons: New York, 1985; pp 180−181.

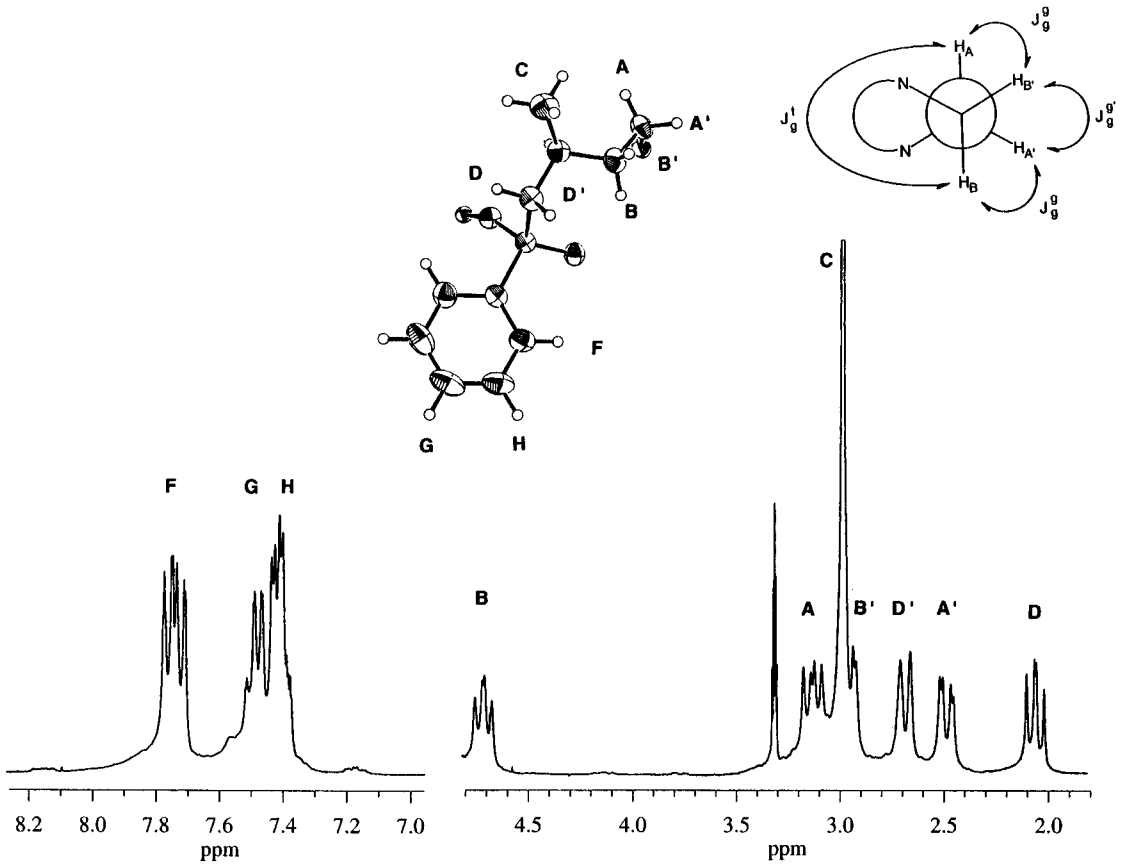

Figure 3. ^{1}H NMR spectrum (300.0 MHz) of $[Al(H_3ppma)_2](NO_3)_3$ in CD_3OD.

couplings based on Pauling electronegativities using the method described by Abraham and Gatti[25] suggests the J_g' values should be in the range of 2−4 Hz, with the J_g^g value being even smaller. The J_t^g value will be large (10−12 Hz) as is also the geminal coupling constant J_{gem} (−10 to −15 Hz). On the basis of these assumptions it is clear that the hydrogens H_A and H_B will possess two large (J_t^g and J_{gem}) couplings and one very small (J_g^g) coupling, and consequently a triplet-like pattern is observed. Hydrogens $H_{A'}$ and $H_{B'}$ will possess one large (J_{gem}), one small (J_g^g), and two very small (J_g^g) couplings and thus appear doublet-like in appearance. The 2D COSY spectrum further confirms these assignments, with clear correlations existing between the geminal pairs of hydrogens and the vicinal hydrogens which are trans to each other. The methylenic hydrogens H_D and $H_{D'}$ show two resonances. On complexing the metal, each phosphorus is rendered chiral and thus the NCH_2P hydrogens become diastereotopic. These are located in two very distinct magnetic environments, and thus the *pro-S* hydrogen ($H_{D'}$) exhibits a doublet-like resonance (*i.e.*, one large coupling $^2J_{HH}$) at higher frequency due to the deshielding of P═O, whereas the *pro-R* hydrogen (H_D) exhibits a triplet-like pattern. The expected pattern for this system would be two doublets of doublets; however, this is clearly not what is observed. There can be no doubt that these two resonances are assigned correctly since they are the only resonances in the 2D COSY spectrum which show only one correlation (*i.e.*, with each other). The rigidity of the complex places the two hydrogens in very different magnetic environments ($H_{D'}$ is close to P═O and H_D is close to P−O−M) resulting in two different values for the couplings to phosphorus ($^2J_{HP}$). One of these is small ($^2J_{HD'P}$) giving rise to the doublet-like resonance, and one is significantly larger ($^2J_{HDP}$) giving rise to the triplet-like resonance.

The ^{13}C{H} NMR spectra consist of eight resonances, the data for which are shown in Table 2. The assignments were made by taking into account the expected coupling patterns and with the aid of ^{13}C APT (attached proton test) experiments. The aromatic carbons all appear in the range of δ 129−135, with each carbon showing coupling to phosphorus. The methylenic carbons appear as a doublet at δ 57−58 due to coupling to phosphorus ($^1J_{PC}$ = 98−101 Hz). The ethylenic carbons occur as singlets at around δ 52 and 58, with the methyl carbons showing small $^3J_{PC}$ coupling (9−10 Hz) at δ 47−48.

The ^{31}P{H} NMR spectra of the complexes show the expected single resonance at a chemical shift of δ 11−16 (Table 2), a lower frequency than observed in the free ligand. In the gallium and indium complexes the expected singlet is observed; however, the aluminum complex exhibits an unusual multiplet. This multiplet is due to a rarely observed phosphorus−aluminum coupling interaction ($^2J_{AlP}$ = 6.7 Hz). With a ^{27}Al nuclear spin of $I = {}^5/_2$, any observable coupling to phosphorus should result in a sextet, and this is indeed what is observed. The coupling pattern should consist of six equidistant resonances separated by $^2J_{AlP}$ of equal intensity but with unequal line widths and therefore unequal peak heights.[26] Four lines are clearly visible, with the outer two lines exhibiting inner shoulders (Figure 4). That this highly unusual coupling phenomenon is observed is a testament to the high symmetry of the complex. Such coupling is unobservable for the gallium and indium complexes, as it should be, due to a combination of high nuclear spins, large nuclear quadrupole moments, and the existence of more than one NMR-active isotope. The corresponding ^{27}Al NMR spectrum (Figure 4) also exhibits this coupling, with a semiresolved septet being observable at δ −12.9 (due to coupling to six equivalent phosphorus atoms) with a line width $W_{1/2}$ = 23 Hz. The line width is remarkably narrow as it stands but, were

(25) Abraham, R. J.; Gatti, G. J. *J. Chem. Soc., B* **1969**, 961.

(26) Delpuech J.-J. *NMR of Newly Accessible Nuclei*; Laszlo, P., Ed.; Academic Press: New York, 1983; Vol. 2, pp 153−195.

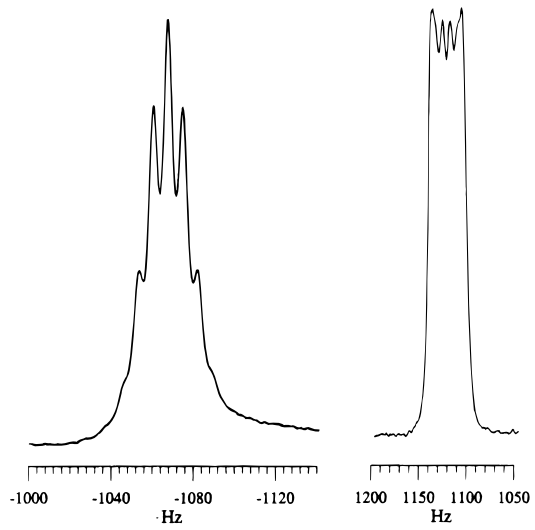

Figure 4. ^{27}Al (78.2 MHz, 50 °C) (left) and ^{31}P (81.0 MHz, room temperature) (right) NMR spectra of $[Al(H_3ppma)_2](NO_3)_3$ in CD_3OD.

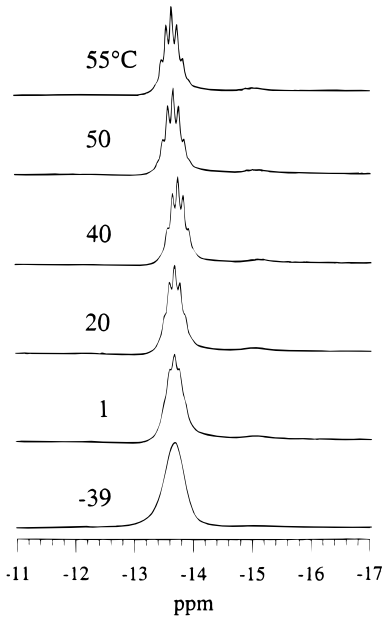

Figure 5. ^{27}Al NMR spectra (78.2 MHz) in the variable temperature study of $[Al(H_3ppma)_2](NO_3)_3$ in CD_3OD.

the coupling not observable, a much narrower line would be observed (*i.e.*, the resonance actually comprises seven much narrower lines!). The septet intensities predicted[26] (1:6:15:20:15:6:1) are observed with the central line and four adjacent lines being clearly resolved (separated by $^2J_{AlP} = 6.7$ Hz) and the remaining outer lines clearly visible as shoulders at the expected height. The appearance of the resonance at low frequency is indicative of an octahedral aluminum complex.[12,26] A variable temperature NMR study of $[Al(H_3ppma)_2](NO_3)_3$ in CD_3OD from −39 to +55 °C (Figure 5) highlights the temperature dependency of line widths for quadrupolar nuclei, where better resolution is observed for the spectrum at 55 °C with the total loss of resolution due to broader line widths at −39 °C. This observation is consistent with the temperature dependency of τ_c, the isotropic tumbling correlation time which decreases with increasing temperature, resulting in a narrowing of the line width ($\tau_c \propto 1/T_{1Q}$).[12b] The ^{71}Ga NMR spectrum of $[Ga(H_3ppma)_2]^{3+}$ exhibits a single resonance at δ −62.3 with a line width $W_{1/2} = 50.0$ Hz, and the ^{115}In spectrum of $[In(H_3ppma)_2]^{3+}$ shows a single resonance at δ −14.7 with a line width $W_{1/2} = 1630$ Hz.

Al(III)−H$_3$ppma Solution Studies. The ^{27}Al NMR spectra of a series of solutions ($R = [L]_T/[M]_T$, L = [H_3ppma] and M = [Al]) in the range $0.24 < R < 3.90$ (where the concentration of aluminum is 24.3 mM) is shown in Figure 6 (left). Three prominent resonances are observed at δ −0.7, −6.9, and −13.1; these correspond to Al ($[Al(H_2O)_6]^{3+}$), AlL ($[Al(H_3ppma)(H_2O)_3]^{3+}$), and AlL_2 ($[Al(H_3ppma)_2]^{3+}$), respectively. The assignments are based on peak intensities when excess ligand is present (AlL_2 is prominent and occurs at a chemical shift identical to that of the isolated complex $[Al(H_3ppma)_2][NO_3]_3 \cdot 2H_2O$) and when excess metal is present ($[Al(H_2O)_6]^{3+}$ is prominent with AlL reaching its maximum intensity). The relative intensities also correlate with their respective ^{31}P NMR spectra. The chemical shifts of the species are of the usual magnitude for octahedral aluminum complexes.[12,26] It is also evident that the shift to lower frequency of $[Al(H_2O)_6]^{3+}$ (δ −0.7) upon complexation with H_3ppma ($3 \times P{-}O^-$) is additive (*i.e.*, addition of one ligand (AlL) induces a shift of −6.2 ppm (δ_{AlL} −6.9) and addition of a second ligand (AlL_2) induces a second shift of −6.2 ppm (δ_{AlL2} −13.1). This type of phenomenon is commonly observed in aluminum complexes.[27]

As R is increased, the consumption of free aluminum is evident and, the intensity of the resonance for Al decreases until it is almost fully consumed at $R = 3.90$. A direct visual comparison with the corresponding ^{31}P NMR spectra (Figure 6 (right)) can be confusing (*i.e.*, at $R = 3.90$, the majority of aluminum is present as AlL_2 and an intense peak is observed in the ^{27}Al NMR spectrum for this species); however, in the corresponding ^{31}P spectrum the most intense resonance corresponds to the free ligand (as this is in excess) which is invisible to ^{27}Al NMR and thus the resonances of the AlL_2 species appear small in comparison. On calculation of the concentrations of the species taken from the integral intensities, however, it becomes clear that the two species are complementary.

The ^{31}P NMR spectrum consists of five prominent resonances at δ 14.3, 15.5, 18.2, 18.5, and 19.6, double the number of resonances observed for the complex in the ^{27}Al NMR spectrum (plus one resonance corresponding to the free ligand). These can be readily assigned by comparison with the ^{27}Al spectra and by the knowledge that, upon complexation, the phosphorus centers are rendered chiral with different diastereomers possible. The narrow resonance at δ 18.5 is that of the free ligand L (H_3ppma), and the two broad resonances at δ 14.3 and 15.5 correspond to the two diastereomers of AlL_2. It is noteworthy that these two appear in the same ratio throughout the titration, and it is thus clear that they are of the same stoichiometry. A broadness of the peaks is also evident, which is not due to exchange processes on the NMR time scale. The broadening of the peaks is mainly due to poorly resolved $^2J_{AlP}$ coupling, coupling which was better resolved in the ^{31}P NMR spectrum of the isolated *RRRSSS* complex. A shift to lower frequency of AlL_2 with respect to L is seen. This was also apparent in the spectrum of the isolated complex. It is likely that these complexes correspond to the above mentioned *RRRSSS* diastereomer along with the less predominant *RRSSSR* diastereomer. The intensity of these resonances diminishes as R is lowered and is mirrored in the ^{27}Al spectra by the concomitant disappearance of the AlL_2 resonance. The remaining two resonances, which become more pronounced when R is low, correspond to the monoligand AlL species (presumably an *RRR*/*SSS* and *RRS*/*SSR* diastereomeric pair) and are slightly obscured by the free ligand resonance L. Again, broadness is observed which is attributable to $^2J_{AlP}$ coupling. The integrals of these peaks give a concentration of AlL which is consistent with that derived from the ^{27}Al spectrum.

The observation of both AlL and AlL_2 species suggests that two equilibria are present in solution (*i.e.*, the formation of the

(27) Finnegan, M.; Lutz, T. G.; Nelson, W. O.; Smith, A.; Orvig, C. *Inorg. Chem.* **1987**, *26*, 2171.

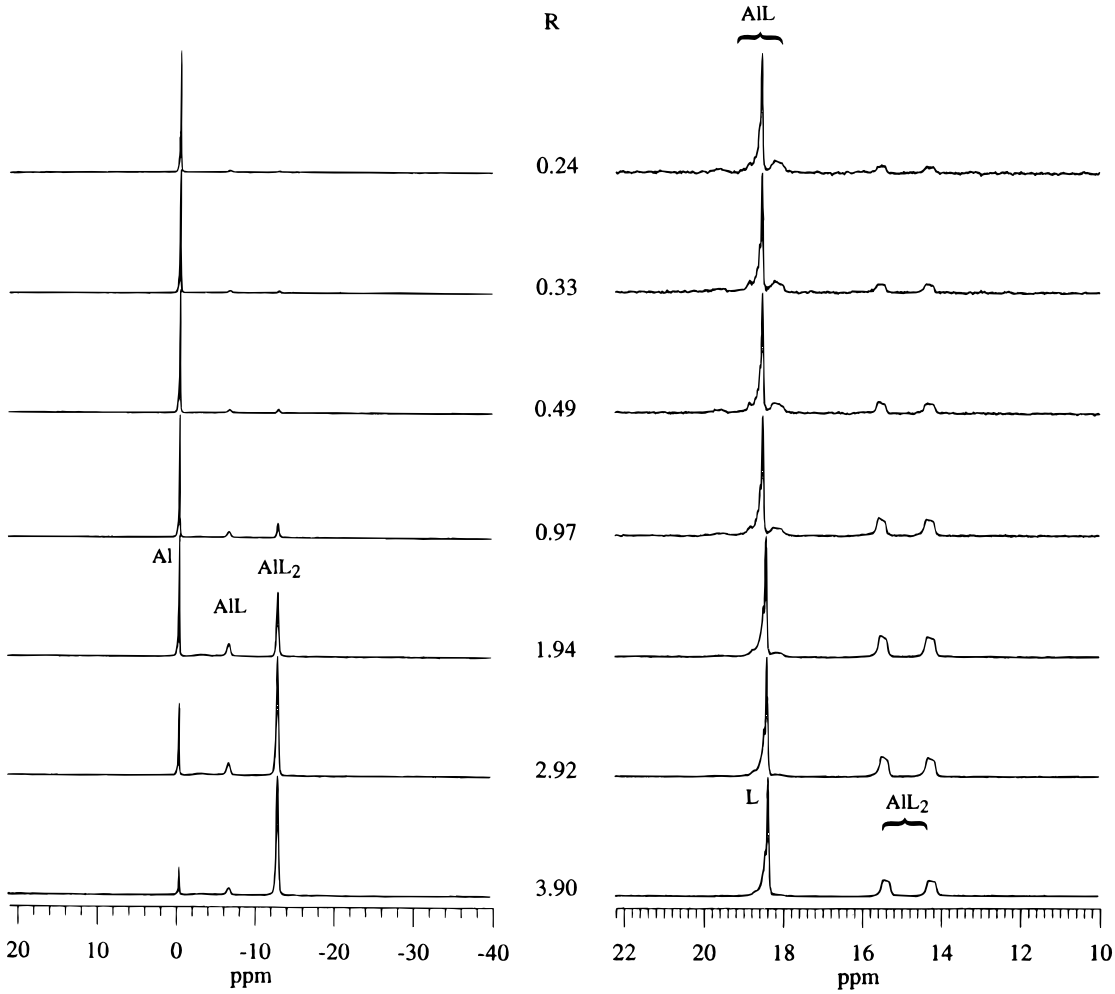

Figure 6. ^{27}Al (78.2 MHz) (left) and ^{31}P (121.0 MHz) (right) NMR spectra for the stability constant study of the Al(III)−H_3ppma system, ($R = [L]_T/[M]_T$).

1:1 and 2:1 complex (eqs 1 and 2) where M = Al(III) and L = H_3ppma).

$$M + L \rightleftharpoons ML \quad (1)$$

$$ML + L \rightleftharpoons ML_2 \quad (2)$$

Integration of both ^{31}P and ^{27}Al spectra allows $\bar{n}$ (the ratio of bound ligand to total metal) to be calculated ($\bar{n} = ([L]_T - [L])/[M]_T$), and from mass balance equations and standard equilibrium constant expressions for β_1 and β_2, $\bar{n}$ can be expressed as eq 3.

$$\bar{n} = (\beta_1[L] + 2\beta_2[L]^2)/(1 + \beta_1[L] + \beta_2[L]^2) \quad (3)$$

A plot of $\bar{n}$ vs [L] is shown in Figure 7 (top). Using eq 3, a calculated curve is produced by varying β_1 and β_2 yielding values of log $\beta_1 = 0.93$ (±0.22) and $\beta_2 = 3.45$ (±0.02).

Ga(III)−H_3ppma Solution Studies. The ^{71}Ga NMR spectra of a series of solutions where $0.24 < R < 3.83$ and the concentration of gallium is 24.8 mM is shown in Figure 8 (left). Two prominent resonances are observed at δ −1.0 and −57.6; these correspond to free gallium Ga ($[Ga(H_2O)_6]^{3+}$) and GaL_2 ($[Ga(H_3ppma)_2]^{3+}$), respectively. Unlike the aluminum system, the GaL monoligand species is barely observable as an insignificant broad resonance and is only seen when R is small, at about half of the shift difference between the Ga and GaL_2 resonances ($\delta \approx -30$), as was the corresponding AlL resonance ($\delta_{AlL} = (\delta_{AlL2} - \delta_{Al})/2$). The chemical shifts observed for the gallium system are indicative of octahedral geometries. The gradual disappearance of the resonance for free gallium (Ga) with the concomitant growth of the resonance for GaL_2 is evident as R is increased. The line width ($W_{1/2} = 93$ Hz) for GaL_2 is broader than that of the isolated complex ($W_{1/2} = 50$ Hz) due to the presence of two *in situ* diastereomers seen in

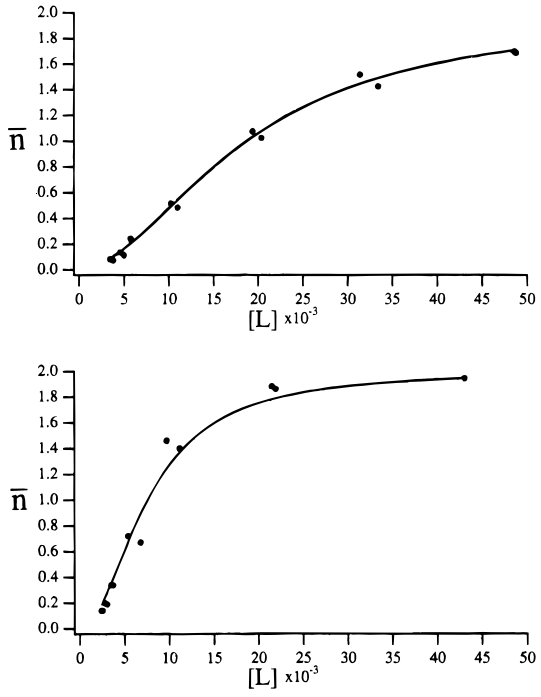

Figure 7. Plot of $\bar{n}$ vs [L] for the Al(III)−H_3ppma (top) and Ga(III)−H_3ppma (bottom) systems (solid lines indicate fits).

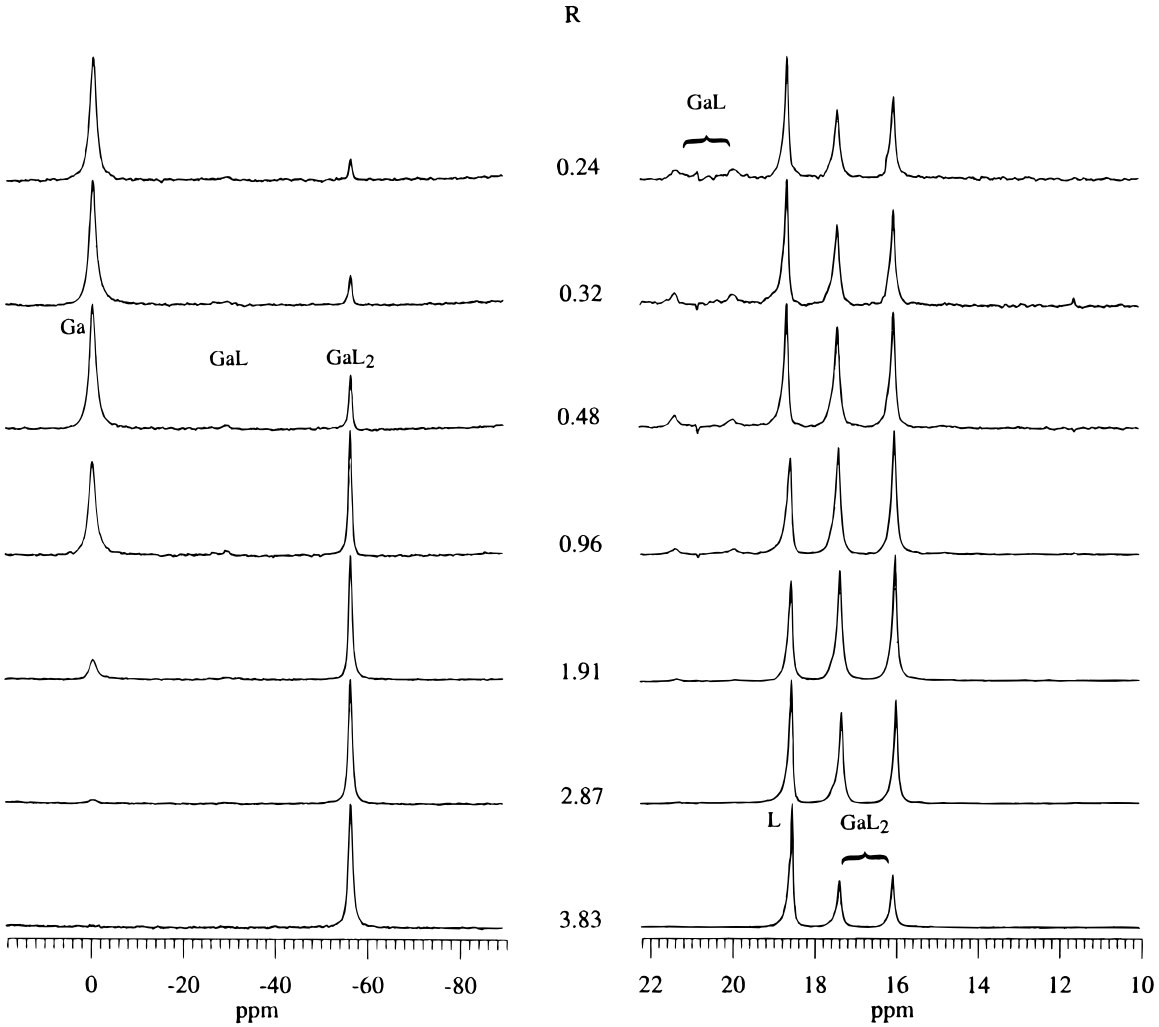

Figure 8. ^{71}Ga (65.7 MHz) (left) and ^{31}P (121.0 MHz) (right) NMR spectra for the stability constant study of the Ga(III)−H_3ppma system ($R = [L]_T/[M]_T$).

the ^{31}P NMR spectrum. In the ^{71}Ga NMR spectrum, these two diastereomers overlap to give the appearance of a single resonance.

The ^{31}P spectra (Figure 8 (right)) consist of three major resonances at δ 16.0, 17.4, and 18.6, the latter corresponding to free ligand, and the former two corresponding to the two diastereomers of GaL_2 (*RRRSSS* and *RRSSSR*). Again, as in the aluminum case, the intensity ratio of these two resonances is invariant. At lower ratios of *R*, an additional two peaks of low intensity are noted (δ 19.9 and 21.3) as were observed in the aluminum case (but with greater intensity); these correspond to diastereomers of the monocapped GaL species. These were of such low relative intensity that they were omitted in the calculation of $\bar{n}$; thus, the formation of GaL_2 can be expressed as eq 4, where M = Ga(III) and L = H_3ppma.

$$M + 2L \rightleftharpoons ML_2 \quad (4)$$

From the integrations of the ^{71}Ga and ^{31}P NMR spectra $\bar{n}$ can be calculated, and from eq 4 and mass balance equations $\bar{n}$ can be expressed as eq 5.

$$\bar{n} = 2\beta_2[L]^2/(1 + \beta_2[L]^2) \quad (5)$$

The plot of $\bar{n}$ vs [L] is shown in Figure 7 (bottom), and using equation 5, the curve can be calculated by varying β_2 to give a value of log β_2 = 4.24 (0.04). The lack of any inflection in the curve between $\bar{n}$ = 0 and 2 also shows that the 2:1 complex is smoothly formed with no evidence for the formation of a 1:1 species.

In(III)−H_3ppma Solution Study. In the study of the indium system, two problems were encountered. First, the use of ^{115}In NMR to probe this system was obviated by the broad line widths of the resonances, compared with their separations. The ^{115}In NMR spectrum of the isolated complex $[In(H_3ppma)_2][NO_3]_3 \cdot 3H_2O$ showed a single resonance at δ −14.6 with line width $W_{1/2}$ = 1630 Hz; however, the resonance for free indium ($[In(H_2O)_6]^{3+}$) occurs at 0 ppm. The separation of −14.6 ppm is only 960 Hz, and thus, the spectra consist of a broad signal comprising overlapping resonances of both In and InL_2. The second drawback was immediately obvious from the ^{31}P NMR spectra (*i.e.*, the bisligand InL_2 complex was fully formed at pH = 1.5). Three resonances were observed at δ 18.5, 18.7, and 19.7, with the first corresponding to free ligand L and the latter two being the two diastereomers of InL_2. As *R* is lowered, the resonance for free ligand (initially in excess) decreased until at a ratio of R ≈ 2 it is no longer visible (*i.e.*, the complex was fully formed). In spite of these problems, a lower limit for the equilibrium constant can be calculated from eq 5 by assuming an NMR detection limit of 2%. Application of this equation to all the ^{31}P NMR spectra yields a lower limit of log $\beta_2 \geq 5.4$.

Discussion

The propensity for tripodal aminophenolates to form bicapped bisligand structures with the lanthanides[1,4] was not observed with the group 13 metal ions, a fact which can probably be attributed to the greater affinity of the latter for nitrogen donors. Instead, completely encapsulated complexes were formed with Al^{3+}, Ga^{3+}, and In^{3+} ions being bound by both oxygen and nitrogen donors. The large tripositive lanthanide ions bond in

a predominately ionic manner,[28] and thus, they show a strong preference for negatively charged oxygen donors to give, in this case, an O_6 donor set. This trend is reflected in the stability constants for such species, where the group 13 metal aminophenolate complex stabilities[29] are several orders of magnitude higher than those for the corresponding lanthanide complexes.[15] On replacing the phenolate donors with the much more acidic phosphinates described herein, the formation of bicapped species with the group 13 metals is now favored. These complexes form at extremely low pH (<2), impossible for the aminophenolates because of the high pK_a values of the phenolate oxygens. At this low pH, encapsulated complexes would not be expected to form because the nitrogens are fully protonated (pK_a values of 6−9); also, because the phosphinate oxygens remain unprotonated even under acidic conditions (pK_a values < 1), bonding exclusively via PO^- results in the bicapped structures similar to those found in the aminophenolate complexes of lanthanides.[15,22]

These bisligand complexes are highly symmetrical with the *RRRSSS* diastereomers being isolated for aluminum, gallium, and indium. The X-ray crystal structure of the indium complex shows exact S_6 symmetry, with the phosphorus atoms of the two hemispheres possessing opposing chirality, (*i.e.*, half R and the other half S). Strong intramolecular hydrogen bonding stabilizes the bicapped structures of the aminophenolate complexes of lanthanides with respect to encapsulated or encapsulated dimeric structures.[22] For the phosphinates, this hydrogen bonding will also impart some stability to the bicapped structures. However, at the low pH studied here, they are unlikely to form encapsulated species. Hydrogen bonding no doubt plays a role in the rigidity of the complexes in solution, as evidenced by the variable temperature ^{27}Al and ^{31}P NMR spectra of the isolated aluminum complex in CD_3OD (up to 55 °C). No broadening or loss of fine structure was observed in the ^{31}P NMR spectrum, whereas the ^{27}Al spectra showed enhanced resolution at higher temperatures.

Aqueous studies reveal a trend in the equilibrium constants which is related to the ionic radii of the metals. Log β_2 for Al < Ga < In increases by approximately 1 order of magnitude each time the group is descended. This may seem somewhat surprising because the smaller harder Al^{3+} ion would be expected to favor bonding to the hard negatively charged phosphinate oxygens (as compared with the larger In^{3+} ion which tends towards an affinity for mixed nitrogen and oxygen donors). Such behavior is observed in the encapsulated complexes of group 13 metals with the tren-based aminophenolates, where (from a possible N_4O_3 donor set) aluminum was found to prefer an N_3O_3, gallium an N_4O_2, and indium an N_4O_3 donor set.[1e] Aluminum shows a preference for all three oxygen donors, whereas gallium tends toward the neutral nitrogen donors with indium sterically able to accommodate all seven donor atoms. What is observed in the complexes of H_3ppma is a much greater affinity for indium, and thus the stability is clearly not dominated only by electrostatic donor atom considerations. It is evident that the size of the metal ion is the dominant factor here, this size discrimination arising from the bulky phenyl groups on the phosphorus atoms. When the bicapped structures are formed, the phenyl groups must be able to fit in between each other, and it is easy to envisage the In^{3+} ion being the ideal size to accommodate all of the phenyls in a relatively strain-free manner. This is highlighted in the X-ray crystal structure of the indium complex, which exhibits perfectly octahedral geometry (O−In−O = 180°, 90.0(1)°).

The ionic radii of the metal ions decrease as the group is ascended (In^{3+} = 0.800 Å, Ga^{3+} = 0.620 Å, Al^{3+} = 0.535 Å),[30] and one can envisage a crowding of the phenyl groups as the phosphinate groups must closely approach each other to bind the metal ion. This crowding results in increasing steric strain and hence the observed lowering of the stability of the complex. Indeed, it is this trend which explains the nonappearance of the monoligand species in the indium system, with only a small amount observable in the gallium case (when gallium is in excess). There is however, a fairly substantial concentration of the monoligand complex in the aluminum system, even when the ligand is in excess. Gallium and indium have favorable ionic radii for forming relatively strain-free bicapped structures, whereas for aluminum more strain is induced and thus the monoligand complex, although still not dominant, is formed in increasing and easily observable amounts.

This still does not explain the anomalous $K_2 \gg K_1$ trend, a phenomenon which has also been observed in the formation of bicapped complexes of the tripodal aminophenolates with lanthanides.[15] Formation constants for stepwise equilibria normally decrease with increasing substitution due to statistical, electrostatic, and steric effects, with few exceptions. The anomalous behavior in the lanthanide aminophenolate complexes was attributed[15] to an entropic effect wherein three waters were displaced in the first step and five waters displaced in the second step. The final complexes were shown by ^{17}O NMR spectroscopy to be seven-coordinate with one bound water. The entropy (as proven in solution calorimetric studies) of that system was greater in the second step, and thus $K_2 > K_1$. For the group 13 metals studied here, it is unlikely that the enhanced stability of K_2 is a result of a change in coordination number because three water molecules will be displaced in each step. The origins of this behavior therefore remain unclear.

The observed rigidity of the bicapped bisligand complexes, coupled with their high symmetry, gives rise to their unusual amenity to study by multinuclear NMR spectroscopy. Of the group 13 metals studied, aluminum offers the most "NMR friendly" nuclear properties. Even so, certain criteria must be met to obtain useful information from ^{27}Al NMR spectroscopy. The line width of a resonance is highly sensitive to both the symmetry about the coordination sphere and the exchange processes. A highly symmetric coordination environment gives rise to a low electric field gradient about the aluminum nucleus, and the relaxation rate is therefore slow, leading to narrow resonances. In asymmetric systems, interaction of the nuclear quadrupole moment with a high electric field gradient results in rapid relaxation and thus broad resonances. The usual range of aluminum line widths in complexes related to the ones reported here can be seen in a few examples: the work of Hegetchweiler[31] and co-workers with inositol-based ligands exhibited line widths $W_{1/2}$ 700 Hz for D_{3d} symmetry aluminum complexes. Polycarboxylate ligands,[32] which are of interest due to their occurrence in natural waters and living systems, give complexes with $W_{1/2}$ in the range of 100−1000 Hz. More comparable with this work is the chemistry of aluminum with biologically relevant phosphates, such as ATP, which give complexes showing line widths $W_{1/2}$ of ∼150−500 Hz; in some cases, sufficient resolution allowed the calculation of association constants at various pH values.[11b−d]

The line widths observed in the H_3ppma−aluminum system are much narrower than in the aforementioned studies, a result of the rigidity and high symmetry of the bicapped complex.

(28) Greenwood, N. N.; Earnshaw, A. *Chemistry of the Elements*; Pergamon: Toronto, 1987; p 1434.
(29) Caravan, P.; Orvig, C. Submitted for publication.
(30) Shannon, R. D. *Acta Crystallogr.* **1976**, *A32*, 751.
(31) Hegetschweiler, K.; Kradolfer, T.; Gramlich, V.; Hancock, R. D. *Chem. Eur. J.* **1995**, *1*, 74.
(32) Orvig, C. *Coordination Chemistry of Aluminum*; Robinson, G., Ed.; VCH Publishers Inc.: New York, 1993; pp 85−121.

These extremely narrow line widths for both monocapped and bicapped species ($W_{1/2}$ = 37 and 23 Hz, respectively, $[Al(H_2O)_6]^{3+}$ = 8 Hz) coupled with a good chemical shift separation allowed a determination of equilibrium constants based on the integrals from combined ^{31}P and ^{27}Al NMR spectra.

^{71}Ga NMR spectroscopic studies are much less common because of the characteristically broad resonances associated with the large nuclear quadrupole moment and low receptivity. To our knowledge, no stability constant determination has ever been made with ^{71}Ga NMR spectroscopy. The only data directly relevant to these studies are those on the macrocycle-based aminophosphinates and carboxylates of Parker and co-workers,[10] where line widths of $W_{1/2}$ = 200−1220 Hz were observed for isolated complexes. The $[Ga(H_3ppma)_2]^{3+}$ line width of $W_{1/2}$ = 50 Hz clearly highlights the difference in symmetry between this complex (O_6 donor set, S_6 symmetry) and the macrocycle-based complexes (N_3O_3 donor set, C_3 symmetry). The difference between O_6 and N_3O_3 coordination is also apparent in the respective chemical shifts of the gallium resonance with the macrocyclic complexes which appear at 130−171 ppm compared to that of $[Ga(H_3ppma)_2]^{3+}$ which appears at −62.3 ppm.

The ^{115}In NMR spectrum of $[In(H_3ppma)_2]^{3+}$ again highlighted the S_6 symmetry. NMR studies of indium complexes belong almost exclusively to the physicist, where studies on solids or melts of indium metals, alloys, and salts have been carried out.[12] Chemical shifts and line widths of solutions of hexaaqua- and tetrahaloindium ions appear to be among the few solution studies reported,[12] with the tetrahedral structures displaying chemical shifts of 200−400 ppm (*c.f.*, $[In(H_2O)_6]^{3+}$, which is used as a reference at 0 ppm). Reported line widths, even for $[In(H_2O)_6]^{3+}$, are in the range of $W_{1/2}$ = 1500−2000 Hz, which makes the line width of $W_{1/2}$ = 1630 Hz (δ −14.7) observed for $[In(H_3ppma)_2]^{3+}$ quite remarkable.

Perhaps the most remarkable discovery in this work was the observed ($^2J_{AlP}$) aluminum−phosphorus coupling. Broad resonances observed in the aluminum−phosphate studies[11b,e] were attributed to such coupling, but no resolution was observed. Such coupling has been observed[33] in highly symmetrical octahedral and tetrahedral solvates of aluminum(III) with phosphate esters and amides such as trimethyl phosphate and hexamethylphosphoroamide. These solvates, and the work reported herein, are the only examples of $^2J_{AlP}$ coupling well resolved in both ^{27}Al and ^{31}P NMR spectra; the coupling constants extracted from both sources were identical. Generally, even in solvated systems, coupling constants are calculated by fitting the line shapes of unresolved resonances to J and T_{1Q} (T_{1Q} = quadrupolar relaxation time). The only report of this coupling calculated in any species remotely resembling a multidentate ligand complex is in the trischelate $[Al(NIPA)_3]^{3+}$ (NIPA = nonamethylimidodiphosphoramide), which is essentially a solvate of the same type as the above mentioned phosphate and phosphoramide solvates.[34] It is unprecedented that well-resolved coupling is observed in both ^{31}P and ^{27}Al NMR spectra of a multidentate ligand complex ($[Al(H_3ppma)_2]^{3+}$). The aforementioned solvates along with the 1:1 adducts, $X_3Al{\cdot}PR_3$ (X = Cl, Br and R = Me, Et)[35] provide one of the few examples of any aluminum−heteroatom coupling ($^2J_{AlP}$ and $^1J_{AlP}$, respectively). In the ^{27}Al NMR spectrum, the partially resolved coupling consists of seven Lorentzian curves at a separation $^2J_{AlP}$, as predicted[34] for the unresolved broad resonances observed by Delpuech and co-workers in $[Al(NIPA)_3]^{3+}$. In a review of ^{27}Al NMR, Delpuech[26] states that such coupling can only be observed with slow exchange and when the quadrupolar relaxation of aluminum is slow ($1/T_{1Q} \ll J$). Usually, coupling constants must be obtained by line shape analysis of unresolved resonances when $J/T_{1Q} \approx 1$. It is unusual to read them directly from resolved spectra, as is demonstrated in this work. The range of $^2J_{AlP}$ coupling constants for the solvates of Delpuech and co-workers[33,34] is 12−30 Hz; however, a much smaller value of 6.7 Hz is obtained for $[Al(H_3ppma)_2]^{3+}$. That there is no system with which to directly compare this value, makes its rationalization difficult, although it must relate to the difference in solvate binding (*c.f.*, a multidentate ligand complex).

Current work is focusing on the chemistry of tripodal tris(aminophosphinato) complexes of the lanthanides and on the effects of varying the phosphorus substituent with respect to solution structures and stability, (*i.e.*, replacing the bulky phenyl group with smaller groups which would not disfavor the formation of aluminum complexes). Incorporation of a more hydrophilic group, such as hydroxymethyl, in place of phenyl has already been achieved and studies are underway to determine the effect of this change on the group 13 metal chemistry. Increased water solubility will enable potentiometric studies to be carried out to investigate the potential formation of encapsulated complexes at elevated pH (the complexes in this study precipitate at pH > 2). Varying the substituents will also shed some light on the anomalous trend in formation constants ($K_2 \gg K_1$) as favorable interactions between adjacent phenyl groups might be a possible contributor to the enhanced stability of K_2 vs K_1.

Conclusion

The formation of highly symmetrical bicapped bisligand complexes of group 13 metals with the ligand H_3ppma has been demonstrated. As a result of the S_6 symmetry of these complexes (as seen in the crystal structure of the indium complex), multinuclear NMR studies were possible with the observation of extremely narrow line widths in the ^{27}Al, ^{71}Ga, and ^{115}In NMR spectra. The aluminum complex showed a rare example of a $^2J_{AlP}$ coupling pattern, observable in both ^{27}Al and ^{31}P NMR spectra. The ligand shows an increased affinity for the larger metals in group 13 at pH = 1.5 in aqueous solutions (β_2 for In > Ga > Al). The preference for indium is attributable to the ionic radii of the metals, indium being of ideal size to accommodate the bulky phenyl groups upon coordination.

Acknowledgment is made to the Natural Sciences and Engineering Research Council (NSERC) and the Du Pont Merck Pharmaceutical Company for operating grants, to Professor J. Trotter for the kind use of his crystallographic facilities, and to Mr. Peter Caravan for his helpful discussions.

Supporting Information Available: Complete tables of crystallographic data, final atomic coordinates and equivalent isotropic thermal parameters, anisotropic thermal parameters, bond lengths, bond angles, torsion angles, intermolecular contacts, as well as tables of observed and calculated structure factors (15 pages). See any current masthead page for ordering and Internet access instructions.

JA961633+

(33) (a) Delpuech, J.-J.; Khaddar, M. R.; Peguy, A. A.; Rubini, P. R. *J. Am. Chem. Soc.* **1975**, *97*, 3373. (b) Delpuech, J.-J.; Khaddar, M. R.; Peguy, A. A.; Rubini, P. R. *J. Chem. Soc., Chem. Commun.* **1974**, 154.

(34) Rubini, P. R.; Rodehüser, L.; Delpuech, J.-J. *Inorg. Chem.* **1979**, *18*, 2962.

(35) (a) Van Vriezen, N. H. W.; Jellinek, F. *Chem. Phys. Lett.* **1967**, *1*, 284. (b) Van Vriezen, N. H. W.; Jellinek, F. *Recl. Trav. Chim. Pays-Bas* **1970**, *89*, 1306. (c) Laussac, J.-P.; Laurent, J. P. *J. Chim. Phys.* **1973**, *70*, 417. (d) Laussac, J.-P.; Laurent, J. P.; Commenges, G. *Org. Magn. Reson.* **1975**, *7*, 72.